Shock Wave Initiation of Pentaerythritol Tetranitrate Single Crystals: Mechanism of Anisotropic Sensitivity

Yuri A. Gruzdkov[†] and Yogendra M. Gupta*[,†]

Institute for Shock Physics and Department of Physics, Washington State University, Pullman, Washington 99164-2816

Received: May 31, 2000; In Final Form: September 16, 2000

A chemical mechanism to explain the observed anisotropy in the shock wave initiation of pentaerythritol tetranitrate (PETN) single crystals is proposed on the basis of semiempirical quantum chemical calculations. Building on the previously proposed model of steric hindrance to shear, the molecular mechanics of shear deformation at the lattice level is correlated with rotational conformations of PETN. The numerous stable conformations of PETN differ in symmetry and dipole moment values. The initial conformation belongs to the S_4 molecular point group and possesses no dipole moment. Because of shear deformations, the molecules change conformations. The [110] shocks result in sterically hindered shear and generate polar conformations. In contrast, the [100] shocks result in little or no polarization. Because the decomposition chemistry of PETN at 5−10 GPa is likely dominated by ionic reactions, local polarity of the lattice plays a crucial role in reactivity. The polar lattice stabilizes the transition state due to dipole−dipole interactions and, thus, facilitates the ionic dissociation. In contrast, the nonpolar lattice results in no stabilization and low reaction rates. Plausible ionic reactions are briefly discussed and experiments are suggested to verify the mechanism proposed.

I. Introduction

Pentaerythritol tetranitrate (PETN; 1,3-propanediol, 2,2-bis-(nitroxy)methyl-, dinitrate (ester)) is a crystalline energetic material used extensively as an initiating or booster high explosive. Because of this application, the sensitivity of PETN to various stimuli has been examined in the past.[1−3] In general, explosive sensitivity is difficult to define because it is both relative and ambiguous. Often, an explosive under investigation is compared to other benchmark explosives whose properties are well-known. The sensitivity of PETN to shock wave compression is intermediate between very sensitive primary explosives, such as lead azide, and less sensitive secondary explosives, such as TNT or RDX.[4]

The role of molecular structure parameters on sensitivity has long been acknowledged.[5] However in 1984, Dick found that under plane shock wave loading the time and run distance to detonation in PETN depended strongly on the direction of shock propagation relative to the crystal axes.[6] In subsequent studies, Dick and co-workers put forward a steric hindrance model in an attempt to explain the observed anisotropic behavior.[7−9] The steric hindrance was correlated to the observed anisotropic, elastic-plastic response arising due to the different slip systems being activated when the crystal is subjected to uniaxial strain deformation along different crystal orientations. Although the model correctly predicted the dependence of the elastic wave amplitude on crystal orientation, it remained largely correlational from the chemical viewpoint. The mechanism relating mechanical properties of the crystal, such as critical shear stress, to chemical reactivity was not understood. Further comments about Dick's model as they pertain to this paper are presented in the next section.

In this work, we use conformational analysis of the PETN molecule to propose a chemical mechanism to explain the anisotropic sensitivity observed for shock wave initiation of PETN crystals. Our calculations are first performed on a single molecule. Then, we qualitatively impose effects of the crystal environment and deformation to obtain insight into the chemical mechanism. This approach, although not rigorous, offers a clear qualitative understanding of the factors governing the strong chemical anisotropy observed in shocked PETN. The results presented provide guidance for future experimental work and set the stage for more rigorous crystal calculations.

The remainder of this paper is organized as follows. Background relevant to this work is in the next section. Section III describes briefly our approach and the computational method used. The results and discussion are presented in section IV and the proposed mechanism is summarized in section V.

II. Background

A. Crystal Structure and Mechanical Properties. The crystal structure of PETN is body centered tetragonal with two molecules per unit cell.[10,11] The unit cell dimensions are $a = 0.938$ nm, $c = 0.671$ nm and the space group is $P\bar{4}2_1c$.[11] Shock compressed PETN displays anisotropic elastic-plastic deformation due to the activation of different slip systems when shocked along different orientations. Several slip systems may be available for a given shock direction; all possible slip systems are given in ref 6. For simplicity, we consider the slip systems that have the maximum resolved shear stress (MRSS) for shock propagation only along the [1$\bar{1}$0] and [100] orientations. These are: $\{100\}\langle 011\rangle$ and $\{110\}\langle 1\bar{1}1\rangle$, respectively. It was assumed that these slip systems are the ones activated in each case.[7]

Because of the elastic-plastic behavior, a shock wave evolves into a two-wave structure as it propagates through the PETN. The amplitude of the faster travelling elastic wave or the elastic precursor depends on the shock propagation direction. For instance, the [110] direction has a significantly larger precursor

[†] E-mail: gruzdkov@wsu.edu; ymgupta@wsu.edu.

10.1021/jp0019613 CCC: $19.00
Published on Web 10/28/2000

than the [100] direction.[12] This property is a manifestation of the mechanical anisotropy in PETN. The elastic precursor amplitude also depends on the input shock stress for the [110] direction.[1,12]

B. Shock Wave Initiation of Detonation. The stress or particle velocity profile behind a shock wave in explosives is not flat, as it would be in an inert material. Instead, the particle velocity or stress amplitude increases with time because of the energy release due to chemical reaction. This increase in stress and particle velocity overtakes the initial shock wave, transforming the shock into a detonation wave.[13] While the evolution of a shock wave propagating along the [110] direction in PETN follows this scenario very well, the [100] direction displays a nearly constant particle velocity behind the shock front similar to inert materials. Moreover, for [100] shocks there was no evidence of a shock to detonation transition in wedge experiments at input stresses as high as 19.4 GPa.[12] In contrast, the [110] direction developed a detonation wave at only 4 GPa. From this large discrepancy Dick and co-workers concluded that use of the conventional thermal explosion model in PETN is not justified.[7]

C. Steric Hindrance Model. The steric hindrance model presented by Dick and co-workers in refs 7 and 9 is an attempt to understand the orientation dependence of shock initiation described above. Under the uniaxial strain conditions imposed by a shock wave, the crystal accommodates plastic deformation through dislocation motion on preferred slip systems. At the lattice level, the net effect of dislocation motion is the transverse displacement of the molecules on one side of the slip plane relative to the molecules on the other side of the plane. The steric hindrance associated with this displacement was emphasized in their model.

The slip (or shear) planes with MRSS for shock propagation along [100] and [110] orientations are shown in Figure 1. The slippage occurs along the shear planes toward the viewer. As can be seen for the [100] shock, the molecules are fairly well separated across the shear planes. This results in relatively easy (or unhindered) slip. In contrast, the molecules overlap across the shear planes for the [110] shock resulting in more difficult (or hindered) slip. The potential energy barrier for shear can be estimated by assuming a potential that describes the energy associated with bond and angle distortions of an individual molecule and with intermolecular interactions. This approach was fairly successful in predicting the relative order of yield stresses (or elastic precursor strengths) for different orientations.[9]

Despite the qualitative success in predicting the mechanical response of the shocked PETN crystals, the use of this model for a mechanistic understanding of the initiation chemistry is not clear. It was suggested[9] that because high potential energy barriers have to be overcome in hindered shear, such a deformation may excite the PETN molecules to very high energy vibrational states or cause direct bond rupture.[7,9,12] This scenario would be highly unconventional in terms of the concepts used in solid-state chemistry to explain chemical reactivity.[14] This fact was pointed out by Jindal and Dlott who argued in favor of a more traditional thermal explanation.[15] They proposed that the orientation dependence could be due simply to the difference in the temperature increase for shock compression along different orientations. Temperature differences may arise due to differences in compressibility, strength, and Gruneisen parameter along each orientation. Our preliminary assessment of anisotropic heating in PETN suggests that the temperature difference between the [110] and [100] orientations is insufficient to explain the very large chemical anisotropy observed experimentally.[16]

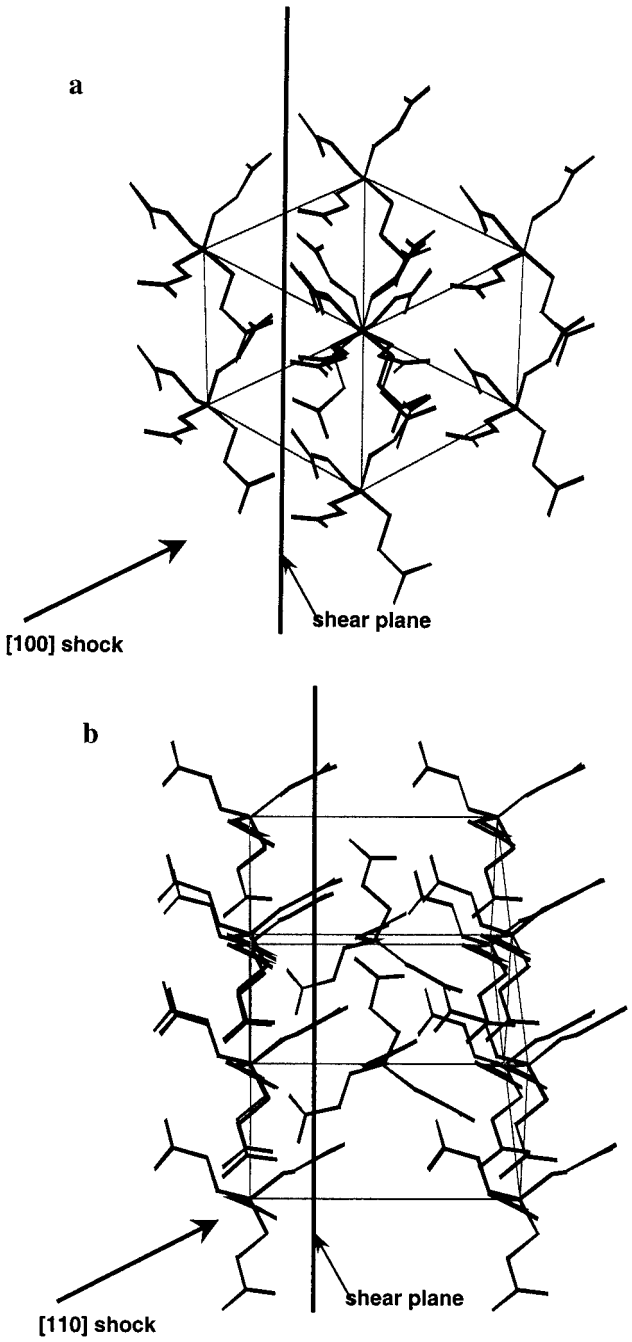

Figure 1. Views of the unit cell of PETN. Molecules at each corner are fully shown. The shear occurs along the shear plane toward the viewer. (a) View of unhindered shear for the [100] shock. (b) View of hindered shear for the [110] shock; two unit cells are shown.

In addition to the two mechanisms described above, an anonymous reviewer has pointed out an alternative mechanism for the observed increase in shock sensitivity for the [110] orientation. The reviewer stated: "*PETN has long been known to react more rapidly in the melt phase, and shear bands are well-known to cause melting and subsequent reaction in other explosive tests, such as impact. If the 110 orientation causes enough resistance to slip, shear bands could be formed which are sufficient size and temperature to cause exothermic reaction after (or as) the PETN melts.*" It is not clear why shear banding would be favored only for the [110] orientation. Also, the proposed mechanism may not be operative on nanosecond time

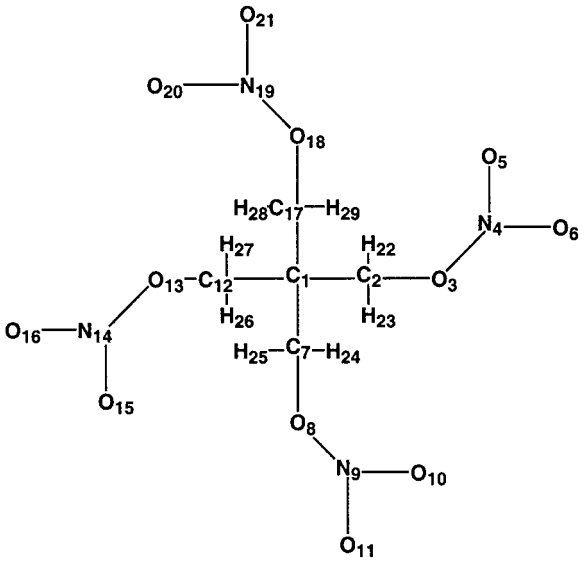

Figure 2. PETN molecule layout for calculations.

scales. Because the reviewer offered no further details or references to support his/her suggestion, it is difficult to discuss a mechanism that has not been published or put forward in definitive terms. We mention it here for the sake of completeness.

In summary, there is no clear mechanism that explains the anisotropic sensitivity observed in shocked PETN single crystals. The results presented below address this issue to provide a plausible chemical mechanism for the observed anisotropy.

III. Approach and Computational Method

Our approach to the problem is based on the notion that steric hindrance leads to large shear stresses that are sufficient to cause conformational changes in PETN molecules. We examine the effect of these changes on molecular properties, such as polarity, charge distribution, etc., using quantum chemical calculations. The computed properties are used to gain insight into the mechanism governing chemical anisotropy. We chose to use a semiempirical approach because it is computationally inexpensive. However, we believe that our approach is adequate for demonstrating the validity of the proposed initiation mechanism concept: *hindered shear leads to conformational changes that result in local lattice polarization that facilitates ionic reactions.*

Calculations were carried out using the commercially available semiempirical molecular orbital program MOPAC.[17] The program implements AM1, PM3, MNDO, and MNDO/d Hamiltonians on a graphical user interface that allows molecules to be rendered as 3D ball-and-sticks models. Geometry optimization and single point calculations were performed for single PETN molecules. The molecular layout used in the calculations is shown in Figure 2.

The first step in the calculations was to choose a Hamiltonian that provided the most accurate molecular geometry of PETN. This was accomplished by using each of the semiempirical methods and comparing the computed geometry with the X-ray data of ref 11. The results are presented in Table 1. As can be seen, AM1 produced the best match to the experimentally measured geometry. The average predictions of the bond lengths from AM1 are within 3.7% of the experimental values compared to those of 4.5 and 3.8% for PM3 and MNDO, respectively; the bond angles are within 1.1% for AM1 compared to 2.1% for the other two methods. Consequently, AM1 was used in the calculations reported below.

TABLE 1: Molecular Geometry of PETN (S_4 Point Group)

		SE Method		
	exp[11]	AM1	PM3	MNDO
	Bond Length, Å			
R(C1,C2)	1.536	1.53	1.55	1.59
R(C2,O3)	1.434	1.45	1.42	1.42
R(C2,H22)	1.03	1.12	1.11	1.12
R(C2,H23)	1.03	1.12	1.11	1.12
R(O3,N4)	1.397	1.35	1.53	1.35
R(N4,O5)	1.222	1.19	1.19	1.21
R(N4,O6)	1.207	1.19	1.18	1.20
	Bond Angle, deg.			
A(C2,C1,C7)	109.2	108.7	108.3	107.8
A(C2,C1,C12)	109.9	111.1	111.9	112.9
A(C1,C2,O3)	107.5	105.4	108.3	108.6
A(C2,O3,N4)	115.9	118.7	117.2	123.1
A(O3,N4,O5)	117.8	117.2	117.9	119.8
A(O3,N4,O6)	113.3	113.0	107.3	113.4
A(O5,N4,O6)	128.8	129.8	134.8	126.8

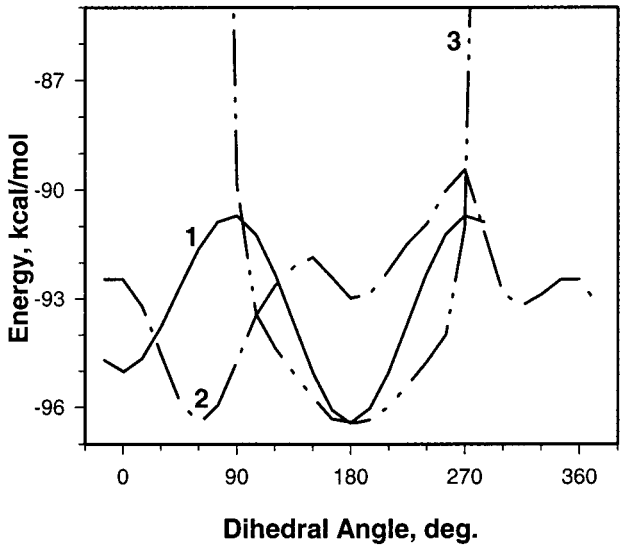

Figure 3. Potential energy of the PETN molecule as a function of rotations about O−N (1), C−C (2), and C−O (3) bonds. The abscissa shows the value of the C2−O3−N4−O6, C7−C1−C2−O3, or C1−C2−O3−N4 dihedrals, respectively. The initial conformation for each rotation is S4.

IV. Results and Discussion

A. Rotational Conformations of PETN. As with most organic molecules in liquid and gaseous states, the PETN molecule is flexible and can change its shape. The molecule can readily go from one conformation to another via internal rotations about single bonds; there are 12 such bonds in PETN. Hence, the electronic ground state of PETN is a 12-dimensional potential energy surface (PES) in the angular space. The most stable conformation of PETN (the global minimum on the PES) belongs to the S_4 molecular point group. Below, this conformation is denoted as S4.

One-dimensional cross sections of the PES for rotations about a C−C, C−O, and an O−N bond are shown in Figure 3. The potential energy barriers for the C−C and O−N rotations are 6.99 and 5.73 kcal/mol, respectively. The full C−O rotation cannot be accomplished one-dimensionally as can be seen from the corresponding PES cross section. However, it can be accomplished if assisted by an additional C−C rotation; the potential energy barrier for this two-dimensional rotation is comparable to the values just indicated.

Because the other bond angles were held fixed, the two minima on the C−C cross section are not true energy minima.

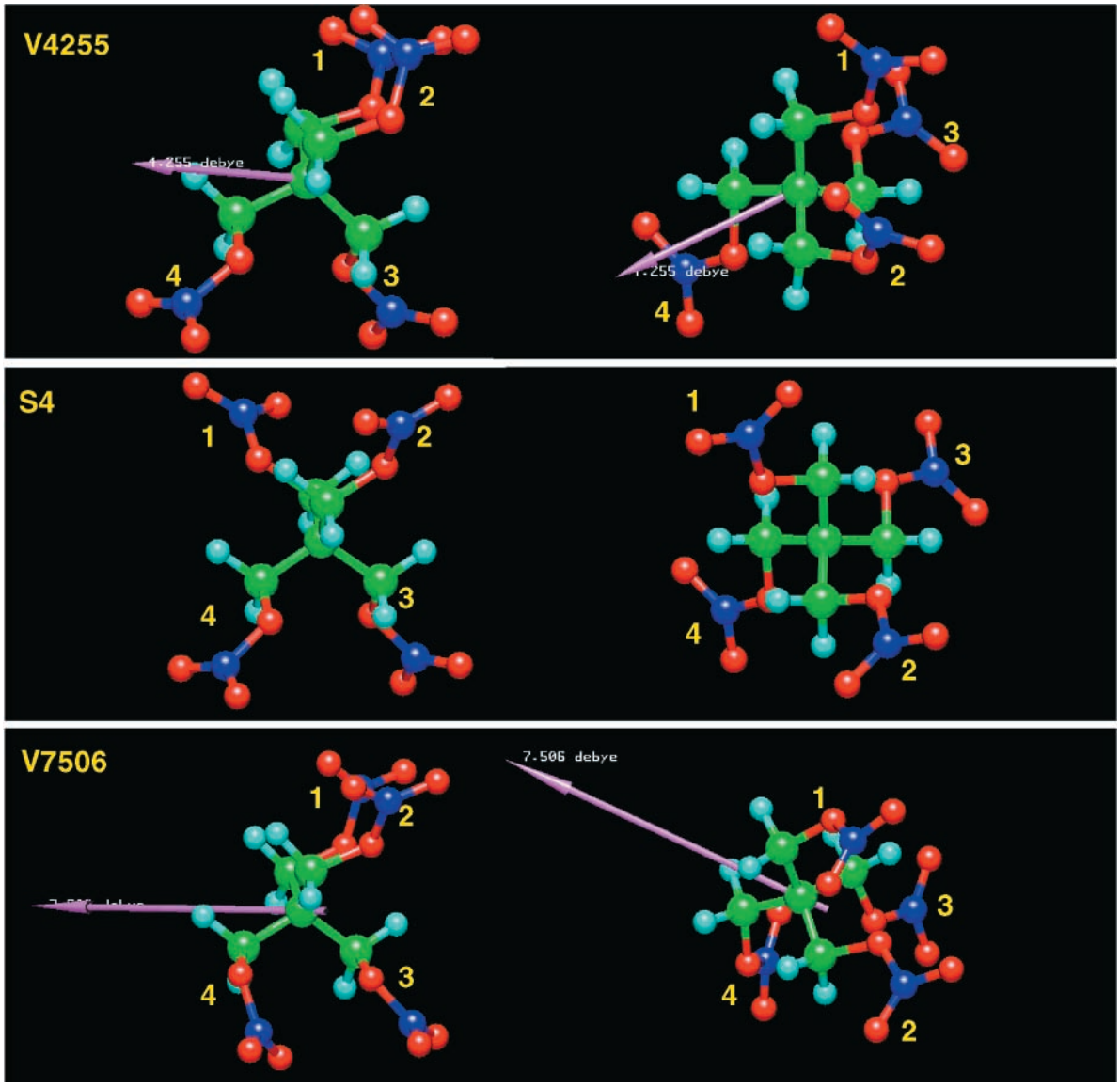

Figure 4. 3D views of three stable conformations of PETN; two orthogonal projections of each conformer are shown. The pink arrows display the dipole vector for each conformer; S4 has a zero dipole moment. Legend: green, carbon; red, oxygen; purple, nitrogen; blue, hydrogen.

The true local minima in the vicinity of these one-dimensional minima can be found by allowing the molecule to "anneal" its geometry, i.e., to change other angles to minimize the energy. The resulting conformations are relatively stable because of the potential energy barrier around the minima. In fact, there are numerous local minima (stable conformations) on the PES whose energies lie within ca. 2 kcal/mol of the global minimum; a typical potential energy barrier is ca. 5 kcal/mol. 3D models of two such conformations that are important to the following discussion are shown in Figure 4 along with the S4 geometry. The geometry of these conformations is summarized in Table 2. More detailed ab initio analyses of these and several additional conformers of PETN will be presented elsewhere.[18]

The conformation denoted as V4255 was obtained from S4 by rotating its one arm (marked 1 in the figure) by 120° about the C−C bond and then annealing the geometry to the local PES minimum. This annealing resulted in an additional 15° rotation about the C−C bond and a large 90° pull of the NO_2 group on the adjacent arm (marked 2 in the figure) toward the first arm via rotation about the C−O bond. The geometry of the other two arms of the molecule remained relatively unperturbed. To obtain the conformation denoted as V7506 from S4, the same procedure was repeated on arms 1 and 3 simultaneously.

The important distinction between these conformations of PETN from S4 is the fact that they have nonzero dipole moments with directions and values depicted by the arrows in Figure 4. The calculated values of the dipole moments are given in Table 3. Each arm of the PETN molecule possesses a relatively large dipole moment. The dipole moment of methyl nitrate, measured to be 2.85 D,[19] would be representative of this value. However, because of the high symmetry of the S_4 point group, the dipole moments of the individual arms compensate each other precisely resulting in a zero net dipole moment. Consequently, perturbations of the S_4 symmetry destroy the compensation and lead to a nonzero dipole moment; one exception is the conformation belonging to the D_{2d} molecular point group. Figure 5 shows the dipole moment changes resulting from the one-dimensional rotations indicated in Figure 3. In Figure 5, it is important to note that the O−N rotation leads to a dipole moment that is significantly less than that of the C−C or C−O rotation. Among the conformers of PETN examined, V7506 possessed the largest dipole moment of 7.5 D. V7506 belongs to the C_2 molecular point group with the

TABLE 2: Calculated Geometry of PETN Conformers

	S4	V4255	V7506		S4	V4255	V7506
ΔH_0, kcal/mol	−96.4	−96.3	−95.9				
point group	S_4	C_1	C_2				
			Bond Length, Å				
R(C1,C2)	1.533	1.531	1.530	*R*(N9,O10)		1.189	1.192
R(C1,C7)		1.534	1.539	*R*(N9,O11)		1.185	1.183
R(C1,C12)		1.539		*R*(C12,O13)		1.452	
R(C1,C17)		1.533		*R*(C12,H26)		1.121	
R(C2,O3)	1.453	1.454	1.452	*R*(C12,H27)		1.123	
R(C2,H22)	1.122	1.123	1.122	*R*(O13,N14)		1.352	
R(C2,H23)	1.122	1.121	1.123	*R*(N14,O15)		1.190	
R(O3,N4)	1.351	1.349	1.351	*R*(N14,O16)		1.185	
R(N4,O5)	1.190	1.190	1.189	*R*(C17,O18)		1.439	
R(N4,O6)	1.185	1.186	1.186	*R*(C17,H28)		1.122	
R(C7,O8)		1.450	1.438	*R*(C17,H29)		1.129	
R(C7,H24)		1.122	1.127	*R*(O18,N19)		1.353	
R(C7,H25)		1.122	1.122	*R*(N19,O20)		1.193	
R(O8,N9)		1.354	1.355	*R*(N19,O21)		1.183	
			Bond Angle, deg				
A(C2,C1,C7)	108.67	111.70	108.12	*A*(O8,N9,O10)	117.19	117.15	117.21
A(C2,C1,C12)	111.09	110.52	111.76	*A*(O8,N9,O11)	112.97	112.78	113.02
A(C2,C1,C17)	108.67	108.80	111.89	*A*(O10,N9,O11)	129.84	130.06	129.76
A(C7,C1,C12)	108.67	105.33	105.02	*A*(C1,C12,O13)	105.39	105.51	112.66
A(C7,C1,C17)	111.09	112.22	111.76	*A*(C1,C12,H26)	111.27	111.43	110.12
A(C12,C1,C17)	108.67	108.19	108.12	*A*(C1,C12,H27)	110.62	110.72	110.25
A(C1,C2,O3)	105.39	105.19	105.90	*A*(O13,C12,H26)	109.17	108.58	101.39
A(C1,C2,H22)	111.27	110.97	111.13	*A*(O13,C12,H27)	109.57	109.81	111.48
A(C1,C2,H23)	110.62	111.04	110.89	*A*(H26,C12,H27)	110.67	110.64	110.65
A(O3,C2,H22)	109.17	110.12	109.63	*A*(C12,O13,N14)	118.67	118.69	120.47
A(O3,C2,H23)	109.57	108.64	108.36	*A*(O13,N14,O15)	117.19	117.15	117.21
A(H22,C2,H23)	110.67	110.72	110.78	*A*(O13,N14,O16)	112.97	112.93	113.02
A(C2,O3,N4)	118.67	118.75	118.61	*A*(O15,N14,O16)	129.84	129.91	129.76
A(O3,N4,O5)	117.19	117.36	117.30	*A*(C1,C17,O18)	105.39	112.64	105.90
A(O3,N4,O6)	112.97	112.95	112.84	*A*(C1,C17,H28)	110.62	110.30	111.13
A(O5,N4,O6)	129.84	129.69	129.86	*A*(C1,C17,H29)	111.27	110.08	110.89
A(C1,C7,O8)	105.39	106.00	112.66	*A*(O18,C17,H28)	109.57	111.59	109.63
A(C1,C7,H24)	110.62	110.99	110.12	*A*(O18,C17,H29)	109.17	101.30	108.36
A(C1,C7,H25)	111.27	111.07	110.25	*A*(H28,C17,H29)	110.67	110.63	110.78
A(O8,C7,H24)	109.57	108.06	101.39	*A*(C17,O18,N19)	118.67	120.41	118.61
A(O8,C7,H25)	109.17	109.60	111.48	*A*(O18,N19,O20)	117.19	117.25	117.30
A(H24,C7,H25)	110.67	110.95	110.65	*A*(O18,N19,O21)	112.97	113.27	112.84
A(C7,O8,N9)	118.67	118.52	120.47	*A*(O20,N19,O21)	129.84	129.48	129.86
			Dihedral Angle, deg				
D(C7,C1,C2,O3)	−58.80	−57.30	171.16	*D*(C2,O3,N4,O5)	−0.30	1.91	2.82
D(C7,C1,C2,H22)	59.41	61.76	−69.85	*D*(C2,O3,N4,O6)	179.77	−178.55	−177.56
D(C12,C1,C2,O3)	60.70	59.61	−73.74	*D*(C1,C7,O8,N9)	176.43	−169.96	−95.09
D(C2,C1,C7,O8)	179.80	−45.93	−47.01	*D*(H24,C7,O8,N9)	57.38	71.00	147.25
D(C2,C1,C7,H24)	−61.85	71.16	65.37	*D*(C7,O8,N9,O10)	0.30	−4.31	3.91
D(C12,C1,C7,O8)	58.80	−165.95	−166.46	*D*(C7,O8,N9,O11)	−179.77	176.48	−175.65
D(C2,C1,C12,O13)	60.70	63.57	76.55	*D*(C1,C12,O13,N14)	−176.43	−171.74	−95.09
D(C2,C1,C12,H26)	178.91	−178.78	−171.06	*D*(H26,C12,O13,N14)	63.97	68.71	147.25
D(C7,C1,C12,O13)	−179.80	−175.64	−166.46	*D*(C12,O13,N14,O15)	−0.30	−1.33	3.91
D(C2,C1,C17,O18)	58.80	49.49	47.67	*D*(C12,O13,N14,O16)	179.77	179.11	−175.65
D(C2,C1,C17,H28)	177.14	174.89	166.66	*D*(C1,C17,O18,N19)	176.43	92.72	170.80
D(C7,C1,C17,O18)	−60.70	−74.64	−73.74	*D*(H28,C17,O18,N19)	57.38	−31.98	50.83
D(C1,C2,O3,N4)	−176.43	171.34	170.80	*D*(C17,O18,N19,O20)	0.30	−5.01	2.82
D(H22,C2,O3,N4)	63.97	51.72	50.83	*D*(C17,O18,N19,O21)	−179.77	174.82	−177.56

TABLE 3: Dipole Moments and ONO_2 Group Charges in PETN Conformers

	S4	V4255	V7506
dipole moment, D	0	4.26	7.51
group charge			
(O3,N4,O5,O6)	−0.2648	−0.2678	−0.2599
(O8,N9,O10,O11)		−0.2525	−0.2391
(O13,N14,O15,O16)		−0.2603	
(O18,N19,O20,O21)		−0.2500	

dipole vector being its natural axis of symmetry. Dipole moments of other conformers ranged from 0.5 to 7.5 D based on the AM1 calculation. The more accurate values obtained using nonlocal density functional calculations (B3LYP/6-31G-(d)) are 3.26 and 5.89 D for V4255 and V7506, respectively.[18]

B. Conformation Change in Shocked PETN Crystal. In contrast to gases and liquids, the flexibility of motion described above is not usually possible in the solid state. Instead, one particular conformation is effectively frozen in. For the PETN crystal, this conformation is S4.[11] The potential energy barriers for rotations in the crystal are significantly higher than those shown in Figure 3. From the data of ref 9, one can estimate it to be ca. 100 kcal/mol.[20] Internal rotations would also require concerted motion of two or more molecules.

During shock wave propagation, significant tangential forces are imparted on the molecules across the shear plane. Because

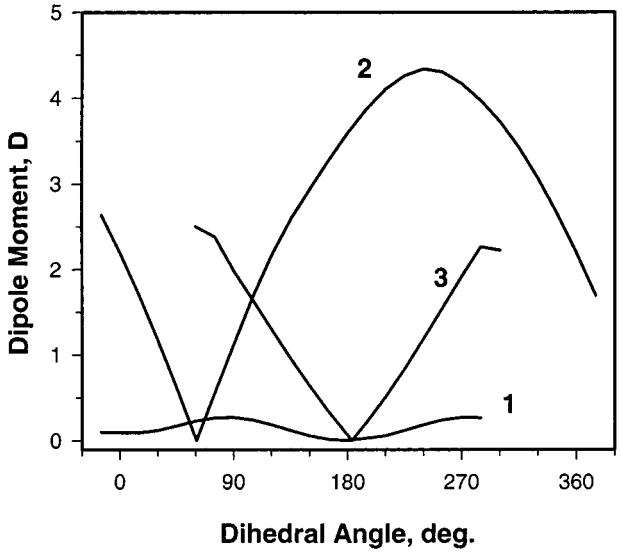

Figure 5. Dipole moment of the PETN molecule as a function of rotations about O−N (1), C−C (2), and C−O (3) bonds; same as in Figure 3.

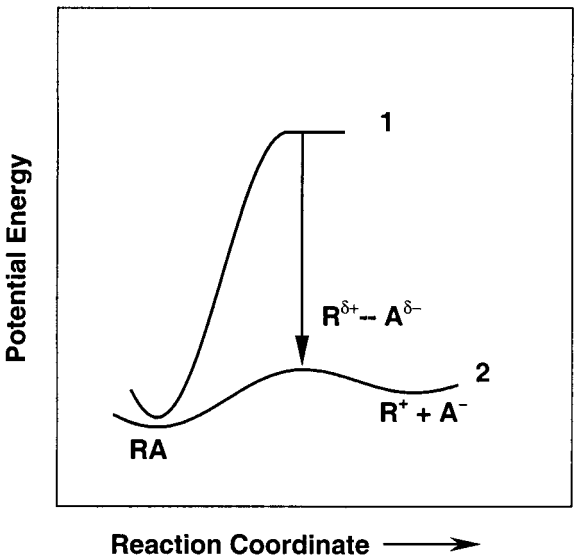

Figure 6. Effect of the crystal lattice on the rate of heterolysis of PETN: nonpolar lattice (1); polar lattice (2). The vertical arrow depicts the large stabilization of the transition state by dipole−dipole interactions. There are no such interactions in the nonpolar lattice.

of these forces, the molecules can deform and change conformations; shear along different slip planes will likely result in different conformations. Molecular mechanics calculations showed that for the unhindered $\{110\}\langle 1\bar{1}1\rangle$ shear only a small rotation of the $-NO_2$ groups about the ester O−N bond is evident while the remainder of the molecules is essentially unperturbed.[9] The calculations described in the preceding section indicate that the molecule distorted in this manner will anneal back to S4. In contrast, during the hindered $\{100\}\langle 011\rangle$ shear the entire arm of PETN that initially overlapped across the shear plane is severely displaced and distorted from its original geometry.[9] The large potential energy barrier for rotation in the crystal mentioned above will prevent the molecules from returning to the initial conformation. Instead, the molecules will anneal to the local potential energy minimum. The resulting conformation is likely to be similar to V4255. After the occurrence of shear deformation, the new conformations will be effectively locked in.

Obviously, more detailed molecular dynamics calculations simulating shear for various shock propagation directions are necessary to determine the exact conformations of PETN produced at the onset of and during inelastic deformation. Qualitatively, however, the difference between the hindered and unhindered shear is such that the former transforms the initially nonpolar crystal of PETN into a polar one, while the latter results in little or no polarization (also, see Figure 5). *Rotational conformations of PETN are the key to this transformation.* Because of the numerous conformers of PETN available on the PES, different types of deformation corresponding to the different shock wave propagation directions, stresses, and loading conditions may result in widely different degrees of polarization. It is important to note that this polarization is microscopic in nature; the net macroscopic polarization will remain zero.

C. Shear-Induced Polarization and Decomposition Chemistry. The dominant reaction of nitrate esters at ambient pressure is homolysis of the $O-NO_2$ bond.[21] Under high pressure, a competing reaction mechanism emerges in which the first step is the formation of a carbocation and the nitrate ion.[22−24] Ionic reactions have a typical activation volume of ca. -20 cm^3/mol and, as such, they are promoted by pressure while homolysis is retarded by pressure.[25,26] The ascendancy of heterolysis over homolysis is gradual with the turning point around 0.5 GPa.[22] Although there are no direct data for PETN it is reasonable to assume that it follows the same pattern as other nitrate esters. The stresses of interest for shock initiation of PETN are on the order of 5−10 GPa, which are well into the heterolytic domain.

The role of the PETN crystal lattice in heterolysis can be best understood using an analogy with the solvent effect well-known in organic chemistry for S_N1 and E1 reactions (see ref 27, for example). The rate-determining step in these reactions is ionic dissociation. In the gas phase or in a nonpolar solvent, the dissociation energy of a typical alkyl halide is 150 kcal/mol. Yet in a polar solvent, the S_N1 heterolysis occurs with an activation energy of only 20−30 kcal/mol.[27] The large reduction in the activation energy arises from the strong stabilization of the transition state and the products by the solvent via dipole−dipole and ion−dipole interactions. In fact, not only does the solvent stabilize the transition state, it pulls apart the incipient ions. It is not uncommon that changing the solvent from polar to nonpolar slows down the reaction by a factor of 10^6 or more.[27]

In the case of PETN, the crystal lattice plays the same role for the reacting PETN molecule that the solvent does in the S_N1 and E1 mechanisms. Therefore, local polarity of the lattice will play a crucial role in reactivity. The polar lattice produced by hindered shear stabilizes the transition state and, thus, facilitates the dissociation. On the other hand, the unhindered shear produces little or no polarization resulting in no stabilization of the transition state and very slow reaction rates. Figure 6 illustrates the effect of lattice polarization on the rate of heterolysis in PETN.

Above, we have analyzed the two extreme cases ([110] vs [100] shock propagation) for chemical anisotropy in shocked PETN single crystals. It is clear from the analysis that other orientations of PETN will fall between these two extremes. In each particular case, the molecular mechanics associated with inelastic deformation at the unit cell level will control the rotational conformations of PETN produced. The conformations, in turn, will determine the local polarity of the lattice and, consequently, the reactivity. Since various conformers of PETN are vastly different in terms of the value of the dipole moment, the polarity of the lattice is expected to vary widely as a function of shock wave direction and loading history. The available

experimental data are consistent with this prediction indicating various degrees of sensitivity to shock waves for different crystallographic orientations.[7]

D. Reaction Mechanism. Although the above considerations imply that the initiation chemistry in PETN under shock compression is ionic, it does not provide the specific chemical mechanism. As mentioned above, on the basis of what is known about the chemistry of nitrate esters, [24] the most plausible initial reaction in PETN is nitrate ion elimination:

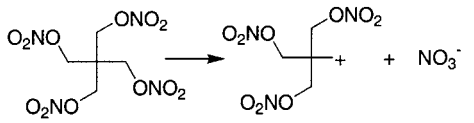

(1)

As can be seen from Table 3, the ONO_2 groups in PETN already carry a significant negative charge. Experimental data for various nitrate esters seem to also indicate that reaction 1 would be the initial decomposition step.[22−24] The carbocation formed in reaction 1 is a primary carbocation. As such, it would be prone to rearrangement to a tertiary carbocation:[27]

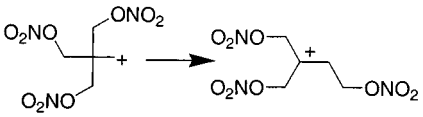

(2)

Reaction 2 is exothermic by about 22 kcal/mol (as estimated using AM1).

Further reactions of the carbocations are far less certain. An attractive possibility is abstraction of the hydride ion from an unreacted PETN molecule. The hydride ion transfer is accompanied by nitronium ion elimination from the PETN molecule to yield the trinitrate aldehyde derivative of PETN; the carbocation transforms into the corresponding alkyl trinitrate. This reaction is exothermic for both the tertiary and primary carbocations by ca. 25 and 38 kcal/mol, respectively. The heat of reaction was estimated using AM1. Since the calculation is essentially a gas phase calculation, the actual values might be appreciably higher. The increase would arise from the difference in the strength of the ion−dipole interactions for the carbocation versus the nitronium ion since the latter is a much smaller molecule. The nitronium ion, NO_2^+, is a strong electrophile known for its high reactivity.[28] It may play an important role in further reaction growth.

E. Experimental Verification. To experimentally detect various conformations of PETN, one needs a method capable of distinguishing between the conformers. The final conformations of PETN differ from the initial one, S4, in two ways: they have a nonzero dipole moment and are of much lower symmetry (typically C_1). Vibrational spectroscopy (Raman and IR) is sensitive to the symmetry of the molecule through selection rules. The 81 genuine vibrational modes of PETN (Γ_g) belong to the following irreducible representations of the S_4 molecular point group: $\Gamma_g = 20\ A + 21\ B + 20\ E$.[18] The 20 A modes are not IR active and the 20 E modes are doubly degenerate.[29] Therefore, one would expect the appearance of new vibrational modes, degeneracy lifting, and a change in the intensity of the overlapped or unresolved modes upon changing the conformation. Work is currently in progress on Raman spectroscopy in shocked PETN crystals to pursue this idea.

Measurements of shock-induced polarization in liquids were successfully carried out in the past.[30] Unfortunately, similar measurements in solids may be difficult. Since the net macroscopic polarization is zero for shear deformation along slip planes, an external electric field would be necessary to partially orient the dipoles to induce the macroscopic polarization that could then be measured. However, the solid matrix usually fixes the molecules with such rigidity that little or no orientation of the dipoles in the external field is possible.[31] In this case, the dielectric constant of the polar crystal would not be different from the nonpolar one. Piezoelectric properties of PETN will further complicate this type of measurement.[16] Other experimental techniques would have to be applied to detect the microscopic polarization.

V. Summary

The chemical mechanism governing anisotropic sensitivity observed for shock wave initiation of detonation in PETN single crystals is proposed on the basis of semiempirical quantum chemical calculations. This mechanism, utilizing the previously proposed model of steric hindrance to shear,[7−9] correlates the molecular mechanics of shear deformation at the unit cell level with rotational conformations of PETN.

There are numerous stable conformations of PETN due to the high flexibility of the molecule. However, this flexibility is severely impaired in the crystal and initially the conformation belonging to the S_4 molecular point group is frozen in. At the onset of plastic deformation for shock compression along particular crystal orientations, significant shear forces are imparted on the molecules across the slip plane. Because of these forces the molecules can change conformations. The new conformations are effectively locked in after the deformation has occurred. Conformers of PETN differ in symmetry and in the value of the dipole moment. The initial conformer of PETN, present at ambient conditions, possesses no dipole moment due to the high symmetry of the S_4 point group. Dipole moments of other conformers range from 0.5 to 7.5 D (AM1 calculations). The presence of polar PETN conformers alters the polarity of the crystal lattice. Because the decomposition chemistry of PETN is likely ionic in the range of 5−10 GPa,[22−24] polarity of the lattice will strongly control the reactivity. The polar lattice stabilizes the transition state due to dipole−dipole interactions and, thus, facilitates the dissociation. In contrast, the nonpolar lattice results in no stabilization and low reaction rates.

The large chemical anisotropy of shocked PETN arises from vastly different degrees of local polarization of the crystal lattice induced by shocks propagating along different crystallographic directions. The initial lattice is not polar. The [100] shocks activate the $\{110\}\langle 1\bar{1}1\rangle$ slip system, which is unhindered. At the unit cell level, the molecular mechanics of shear deformation results in only small perturbations of the molecular geometry leading to little or no polarization. In contrast, the [110] shocks activate the sterically hindered $\{100\}\langle 011\rangle$ slip system. As a result, the geometry of the PETN molecules that overlapped across the shear plane is severely distorted generating polar conformations. This, in turn, transforms the initial nonpolar lattice into a polar one that promotes ionic dissociation. Plausible ionic reactions are briefly discussed and experiments are suggested to verify the mechanism proposed.

Acknowledgment. Dr. J. M. Winey is thanked for sharing his preliminary results on the equation of state of PETN. Drs. Z. A. Dreger and J. J. Dick are thanked for many useful discussions throughout the course of this work. This work was supported by ONR grants N000149310369 and N000149911014.

References and Notes

(1) Halleck, P. M.; Wackerle, J. *J. Appl. Phys.* **1973**, *47*, 976.
(2) Dick, J. J. *J. Appl. Phys.* **1982**, *53*, 6161.

(3) Luebcke, P. E.; Dickson, P. M.; Field, J. E. *J. Appl. Phys.* **1996**, *79*, 3499.

(4) Dobratz, B. M.; Crawford, P. C. *LLNL Explosives Handbook: Properties of Chemical Explosives and Explosive Simulants*; University of California: Livermore, CA, 1985.

(5) Cheret, R. *Detonation of Condensed Explosives*; Springer-Verlag: New York, 1993; p 113.

(6) Dick, J. J. *Appl. Phys. Lett.* **1984**, *44*, 859.

(7) Dick, J. J.; Mulford, R. N.; Spencer, W. J.; Pettit, D. R.; Garcia, E.; Shaw, D. C. *J. Appl. Phys.* **1991**, *70*, 3572.

(8) Dick, J. J. *Munitions Technol. Devel.* **1993**, 14.

(9) Dick, J. J.; Ritchie, J. P. *J. Appl. Phys.* **1994**, *76*, 2726.

(10) Booth, A. D.; Llewellyn, F. J. *J. Chem. Soc.* **1947**, *1947*, 837.

(11) Cady, H. H.; Larson, A. C. *Acta Crystallogr.* **1975**, *B31*, 1864.

(12) Dick, J. J. *J. Appl. Phys.* **1997**, *81*, 601.

(13) Dremin, A. N. *Toward Detonation Theory*; Springer: New York, 1999.

(14) West, A. R. *Solid State Chemistry and its Applications*; John Wiley & Sons: New York, 1984; p 666.

(15) Jindal, V. K.; Dlott, D. D. *J. Appl. Phys.* **1998**, *83*, 5203.

(16) Winey, J. M.; Gupta, Y. M. Unpublished.

(17) Fujitsu Ltd. *WinMOPAC v2.0 for Windows 95 and Windows NT 4.0*, 1997−1998.

(18) Gruzdkov, Y. A.; Gupta, Y. M. *J. Phys. Chem. A*, manuscript in preparation.

(19) Smyth, C. P. *Dielectric Behavior and Structure*; McGrow-Hill: New York, 1955; p 288.

(20) Reference 9 gives an estimate for the energy associated with the hindered shear of 2 kcal/(mol Å^2). Given the unit cell area of 70−100 Å^2, one obtains the barrier value of ca. 140−200 kcal/mol. This value is composed of two terms: the repulsive term of the Lennard-Jones potential and the barrier for internal rotations.

(21) Hiskey, M. A.; Brower, K. R.; Oxley, J. C. *J. Phys. Chem.* **1991**, *95*, 3955.

(22) Naud, D. L.; Brower, K. R. *J. Org. Chem.* **1992**, *57*, 3303.

(23) Davis, L. L.; Brower, K. R. *J. Phys. Chem.* **1996**, *100*, 18775.

(24) Davis, L. L. Reactions of Organic Compounds in Explosive-Driven Shock Waves. Ph.D. Dissertation, New Mexico Institute of Mining and Technology, 1996.

(25) Asano, T.; le Noble, W. J. *Chem. Rev.* **1978**, *78*, 407.

(26) Klarner, F.-G.; Diedrich, M. K.; Wigger, A. E. In *Chemistry under Extreme or Non-Classical Conditions*; van Eldik, R., Hubbard, C. D., Eds.; Wiley: New York, 1997; p 103.

(27) Morrison, R. T.; Boyd, R. N. *Organic Chemistry*, 5th ed.; Allyn and Bacon: Boston, 1987; Chapters 5−7.

(28) Sidgwick, N. V. In *The Organic Chemistry of Nitrogen*, 3rd ed.; Millar, I. T., Springall, H. D., Eds.; Clarendon Press: Oxford, U.K., 1966.

(29) Cotton, F. A. *Chemical Applications of Group Theory*; Wiley: New York, 1990.

(30) Yakushev, V. V.; Nabatov, S. S.; Dremin, A. N. *Sov. Phys.-JETP* **1976**, *42*, 646.

(31) Smyth, C. P. *Dielectric Behavior and Structure*; McGrow-Hill: New York, 1955; p 132.